4ème Conférence Internationale des Energies Renouvelables (CIER-2016)
Proceedings of Engineering and Technology – PET
Vol.17, pp.1- 7

Effect of multiple obstructions on natural convection heat transfer in a vertical channel

Olfa Mechergui[1], Xavier Chesneau[2], Ali Hatem Laatar[3]

LETTM, Département de physique 7021 Jarzouna- Université de carthage
Faculté des Sciences de Bizerte, 7021 Jarzouna Bizerte, Tunisie
[1]olfaamechergui@gmail.com
[3]ahlaatar@gmail.com

LAMPS, Université de Perpignan Via Domitia
52 Avenue Paul Alduy, 66860 Perpignan, France
[2]chesneau@univ-perp.fr

***Abstract*—**In this paper, a numerical study is performed in order to analyze the effect of an adding of obstructions to a vertical open channel on natural convection. The channel is heated asymmetrically with a uniform heat flux. The computational procedure is made by solving the unsteady two dimensional Navier-Stokes and energy equations. This nonlinear system is integrated by a finite volume approach and then solved in time using the projection method, allowing the decoupling of pressure and velocity. More than hundred simulations are performed to determine the best positions and numbers of the obstructions that enhance the induced mass flow and the heat transfer rate for modified Rayleigh numbers ranging from $Ra_m=10^2$ to $Ra_m=10^5$. The numerical results (velocity, pressure, temperature fields and average Nusselt number) provide detailed information about the evolution of the flow structure according to the geometry considered in this study. In addition, they permit to explain why the mass flow rate and Nusselt number are enhanced for certain positions and number of the obstructions. Finally, appropriate correlations have been proposed for determining the optimal configurations and the corresponding enhancement of the mass flow rate and the heat transfer coefficient.

I. Introduction

Natural convection in vertical channel has been extensively investigated both numerically and experimentally. Due to modern engineering applications such as solar collectors, passive ventilation of buildings, cooling of electronic equipments and nuclear reactors, there is a renewed interest in the study of natural convection in vertical channels.

One of the first experimental studies of natural convection in a vertical channel is that of Elenbaas [1] that has identified the different flow patterns according to a modified Rayleigh number Ra_m. This parameter is essentially the classical Rayleigh number divided by the aspect ratio of the channel.

The first numerical solution for developing natural convection flow in an isothermal channel was carried out by Bodia and Osterle [2] using the boundary layer approximation. The authors assumed uniform velocity and temperature profiles and ambient pressure at the channel inlet while postulating fully developed flow at the channel outlet. Laminar natural convection flow in channels with asymmetrical heating was theoretically and experimentally studied. Further studies regarding natural convection in vertical channels are those presented by Vajravelu and Sastri [4], Sparrow [5], Webb and Hill [6], Naylor et al. [7]. To enhance the limited heat transfer performance of a heated vertical channel, several modified configurations of the simple channel have been studied numerically and experimentally. Some authors append two parallel insulated plates at the channel inlet or outlet, as in the studies by Lee [8] and Campo et al. [9].

Others have added an adiabatic chimney downstream of the heated channel, as Haaland and Sparrow [10], Oosthuizen [11], Morrone and Manca [12], Auletta et al. [13], Auletta [14] and Andreozzi [15].

One of the attractive ideas to improve the channel performances is the introduction of internal objects, as auxiliary plates [16, 17] or obstructions [18, 19]. This type of studies is infrequent in the literature.

Kim and Boehm [20] investigated numerically the combined free and forced convective heat transfer from multiple rectangular wall blocks in vertical channels. Studies on mixed and natural convection in channels with single obstruction can be found in references. [21-23]. Mehrotra and Acharya [24] conducted an experimental study of natural convection heat transfer in smooth or ribbed vertical channels. From the above discussion, it can be seen that there is a necessity to study compound effect of multiple obstructions, obstructions on both walls of the channel, aspect ratio of channel and location of the obstruction. The present numerical study is aimed at studying the effect of the aforesaid factors on the rate of heat transfer.

In our paper, a numerical simulation of natural convection in a vertical corrugated channel is performed. The channel is heated asymmetrically at uniform heat flux. Thermal and dynamic aspects of the problem are studied by varying the

ISSN 2356-5608

width and the height of the obstructions while the channel aspect ratio is kept fixed. The main objective of this work is to determine the optimal configurations that maximize the mass flow rate and the average Nusselt number and to propose appropriate correlations for these quantities. The flow structure and the pressure field are also analyzed to explain the system responses for different geometrical parameters and various Rayleigh numbers.

II. Problem Formulation

The aim of this paper is to study numerically the natural convection in an asymmetrically heated vertical channel with obstructions.

Fig. 1 schematically shows the two-dimensional physical system. The studied configuration is composed of two parallel plates forming a vertical channel in which the air can circulate. A portion of the left wall (H/2<Z<3H/2) containing a rectangular protuberance. The wall containing the protuberance is assumed to be heated at uniform heat flux q while the other wall is assumed to be adiabatic. The height of the channel plates is 2H whereas the distance between them is d.

All the thermo physical properties are assumed to be constants, except for the density in the buoyancy force term which can be adequately modeled by Boussinesq approximation. The conservation equations describing the flow are the unsteady 2D Navier-Stokes equations and the energy equation for a constant property incompressible fluid.

:

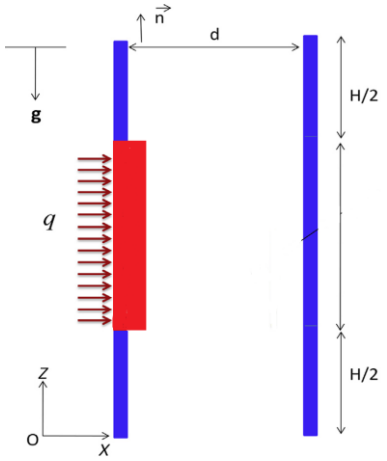

Fig. 1 Geometric configuration

For the flow considered here, the basic governing equations are written in dimensionless form as follows:

$$\frac{\partial U^*}{\partial X^*}+\frac{\partial W^*}{\partial Z^*}=0$$

$$\frac{\partial U^*}{\partial \tau^*}+U^*\frac{\partial U^*}{\partial X^*}+W^*\frac{\partial U^*}{\partial Z^*}=-\frac{\partial P^*}{\partial X^*}+\Pr\left(\frac{\partial^2 U^*}{\partial X^{*2}}+\frac{\partial^2 U^*}{\partial Z^{*2}}\right)$$

$$\frac{\partial W^*}{\partial \tau^*}+U^*\frac{\partial W^*}{\partial X^*}+W^*\frac{\partial W^*}{\partial Z^*}=-\frac{\partial P^*}{\partial Z^*}+\Pr\left(\frac{\partial^2 W^*}{\partial X^{*2}}+\frac{\partial^2 W^*}{\partial Z^{*2}}\right)+\Pr Ra T^*$$

$$\frac{\partial T^*}{\partial \tau^*}+U^*\frac{\partial T^*}{\partial X^*}+W^*\frac{\partial T^*}{\partial Z^*}=\left(\frac{\partial^2 T^*}{\partial X^{*2}}+\frac{\partial^2 T^*}{\partial Z^{*2}}\right)$$

The governing dimensionless parameters appearing in the above equations are the Rayleigh number, the Prandtl number and the modified Rayleigh number.

$$Ra=\frac{g\beta q d^4}{\nu\alpha\lambda}\ ,\ \Pr=\frac{\nu}{\alpha}\ ,\ Ra_m=Ra\left(\frac{d}{h}\right)$$

A. Boundary conditions

The Navier-Stokes equations are solved by imposing the boundary conditions given in the following:

- After and before the protuberance:

$W^*=U^*=0$ and $\frac{\partial T^*}{\partial X^*}=0$

At the protuberance: $\frac{\partial T^*}{\partial X^*}=-1$

- At the inlet and the outlet (0<X<1 and Z=0 or Z=2H/d):

if $W<0$: $\frac{\partial W^*}{\partial Z^*}=\frac{\partial U^*}{\partial Z^*}=\frac{\partial T^*}{\partial Z^*}=P^*=0$

if $W>0$: $\frac{\partial W^*}{\partial Z^*}=U^*=T^*=0$; $P^*=-0.5\left(\frac{1}{\Delta}\int W^* dX^*\right)$

The local Nusselt number of the heated wall can be evaluated from equation:

$$Nu_z=\frac{h(z)d}{\lambda}=\frac{1}{T^*(z)}$$

The dimensionless overall heat transfer rate is represented by the average Nusselt number and defined as:

$$Nu_z=\frac{d}{H}\int_{H/2d}^{3H/2d} Nu(z)\ dz$$

III. Numerical Resolution

The calculation has been performed using an in-house written Navier-Stokes solver, which was initially developed at LIMSI (France) and then was adapted for the time integration of the above system of equations. This code has been successfully used for different types of problems [25-28].

The unsteady Navier-Stokes equations are discretized in space by the finite volume method. The time integration is performed using a time-splitting algorithm, also known as a prediction-projection algorithm, which allows one to decouple pressure from velocity. Assuming all quantities known at time $n\Delta T$, the solution at time $(n+1)\Delta T$ is obtained as follows:

An intermediate velocity field V^* is first computed using a second-order time scheme. This time stepping combines a second order backward Euler scheme for the diffusion terms,

ISSN 2356-5608

with an explicit second-order Adams-Bashforth extrapolation for the non-linear terms, taking into account known pressure field. This step reads:

$$\frac{3V^{*}-4V^{N}+V^{N-1}}{2\Delta\tau}+2(V.\vec{\nabla}V)^{n-1}-(V.\vec{\nabla}V)^{n-1}=-.\vec{\nabla}P^{n}+\mathrm{Pr}\Delta V^{n}$$

In the second step, this intermediate velocity field is projected onto the subspace of divergence free vector field using the Helmholtz decomposition theorem. This step reads:

$$V^{n+1}-V^{n}=\frac{-2\Delta\tau}{3}\vec{\nabla}(P^{n+1}-P^{n})$$

It is accomplished by taking the divergence of equation giving rise to a Poisson's type equation for the incremental pressure:

$$\Delta\theta=\frac{3}{2\Delta\tau}\overrightarrow{\nabla V^{n}}\ ;\ \Delta\theta=P^{n+1}-P^{n}$$

This equation is solved with a multigrid algorithm, in which the presence of internal blockings is automatically taken into account.

Once the pressure field is obtained, the new quantities at $(n+1)\Delta T$ are given by:

$$P^{n+1}=\theta+P^{n}$$

$$V^{n+1}=V^{*}-\frac{2\Delta\tau}{3}\overrightarrow{\nabla\theta}$$

The space discretization uses a centered scheme for the diffusive fluxes and a second order upwind finite difference method by means of a Quadratic Upstream Interpolation Convective Kinematics (QUICK) scheme for the convective terms.

The computations were performed on a 2D computational domain restricted to the space between plates, excluding the entrance and exit regions outside the channel and using a special treatment of the inlet and outlet sections of the channel. The computational domain is $X^{*}Z^{*}$ where $X^{*}=1$ and $Z^{*}=2H/d=10$.

The spatial discretization used was an 82 * 258 non-uniform grid that is refined near the walls. The time step is fixed at $\Delta T=5*10^{-6}$, close to the stability limit.

In order to ensure the accuracy of the numerical results, a grid dependence study was realized. Computations were carried out with three gridlines systems, i.e. 82 * 258, 162 * 258 and 82 * 514 with $Ra_{m}=10^{-5}$. The changes in the mesh size give errors less than 2% in the relevant parameters such as the mass flow rate and the average Nusselt number. Therefore, 82 * 258 gridlines system is suitable and used throughout the present work.

A. Validation of the results

To verify the accuracy of our results, comparisons with numerical and experimental results available in literature are given in the following.

Firstly, the problem treated experimentally by Webb and Hill [6] was simulated in the present work.

Fig. 2 displays a comparison between the average Nusselt numbers obtained numerically in our work and the experimental ones given in Ref. [6], for different modified Rayleigh numbers ranging from 10^{2} to 10^{6}. As can be seen, the agreement between the numerical and experimental results is good.

The second validation concerns the comparison with numerical results obtained by S. Habchi and S. Hacharya in vertical channel with partial rectangular obstruction.

Fig. 3 show the streamlines in the channel for a block height H / L = 0.1, a Reynolds number Re = 1195. And a Richardson number were tested Ri = 0.1. The structure of the flow provided by our code is almost similar to that found by Habchi and Acharya.

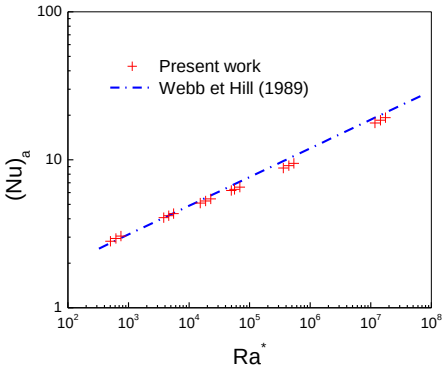

Fig. 2 Average Nusselt number as a function of modified Rayleigh number

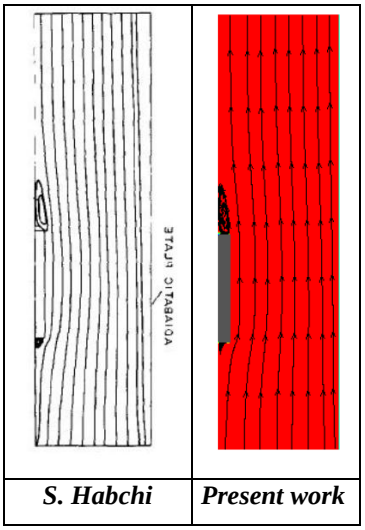

Fig. 3 Streamlines Re=1195, H/L=0.1, Gr/Re^{2} =0.1

IV. Results and Discussion

The problem addressed here is deceptively simple, because the numerical modeling of the natural convection flows in vertical open channels is difficult (even in the 2D case) mainly when the computational domain is restricted to the channel geometry.

ISSN 2356-5608

Only the outlet conditions can be imposed, because the boundary conditions at the inlet are unknown and are determined by what happens close to the heated source located downstream to the entrance. This difficulty has generally led people to consider homogeneous Neumann boundary conditions. The determination of the exact boundary conditions to be imposed at the entrance of the channel is an open problem that has not yet been solved.

Le Quéré [29] is among the few scientists having provided a satisfactory answer to this type of problem. He performed singular value decomposition (SVD) of the discrete Stokes operator that arises from the discretization of the governing Navier-Stokes equations, using the classical staggered grid formulation. He has shown that the imposition of Neumann type boundary conditions may lead to one or several non trivial combinations of velocity- pressure fields which satisfy the homogeneous Stokes operator, in addition to the unavoidable constant pressure mode. He proposed an algorithm in which the solution is sought as a combination of particular solution of the inhomogeneous Stokes or unsteady Stokes problem and a linear combination of the modes of the kernel so as to satisfy global conditions such as a mean pressure difference between outlet and inlet.

In the present study, we will use flow conditions identical to those of the Benchmark exercise [19].

Fig. 4 displays the time variation of the non-dimensional mass flow rate for different modified Rayleigh numbers ranging from $Ra_m=10^2$ to $Ra_m=10^5$. It is seen that curves have the same shape and the mass flow rate increases with the modified Rayleigh number. We note that the mass flow rate tends to a constant value after the damping of the transient effect, and the laminar steady state becomes established.

Fig. 5 illustrates the vertical velocity profiles at the entrance of the heated plate for various modified Rayleigh numbers ($Ra_m= 10^2, 10^3, 10^4, 10^5$). At the entrance, the velocity profiles are approaching the fully developed parabolic profiles for the four different values of Ra_m. We also notice that the velocity peak is slightly asymmetric and it increases with the modified Rayleigh number Ra_m.

Fig 6 depict the vertical velocity profiles at the exit of the heated wall of the channel outlet for various modified Rayleigh numbers. The velocity profiles are of a boundary layer type with a strong asymmetry highlighted by the acceleration of fluid near the heated wall.

Negative velocities are observed near the adiabatic wall corresponding to the reversal zone. When the Rayleigh number increases, the velocity peak increases too and moves toward the heated wall, due to the fluid acceleration, causing the reduction of the boundary layer thickness.

The improvement of the mass flow rate in the channel is show in Table 1.

Comparing these results with those of a single channel of the same size and under the same boundary conditions, we find that the mass flow rate in a grooved channel is higher than in a simple channel (M = 78.39).

Fig 7 shows the streamlines for different values of the modified Rayleigh number. We note, for a modified Rayleigh number equal to $Ra_m = 10^3$, that streamlines are parallel to the channel axis. Therefore, we do not observe the phenomenon of penetration of the channel output unlike other values of the modified Rayleigh number. Indeed, from the modified Rayleigh number equal to $Ra_m = 10^4$ a recirculation zone appears on the side of the adiabatic wall of the channel, it increases in size when the Rayleigh number believes.

When the Rayleigh number increases, the fluid in the thermal boundary layer is accelerated. This boundary layer must be constantly powered by the creation of an air intake at the bottom of the channel which causes a folding of the streamlines on the side of the hot wall. A vacuum zone is established along the adiabatic wall of the channel that will be invaded by the fluid from the outside which will penetrate through the upper opening of the channel.

Fig. 8 represents the values of average Nusselt for the geometrical configuration of reference where the heated portion is composed of five rectangular grooves. In general, when setting the height h of the grooves, we note that the average Nusselt number increases with the modified Rayleigh number. On the other hand when setting the modified Rayleigh number, the average Nusselt decreases with height h of the grooves.

Fig. 9 shows the variation of the average Nusselt number for different numbers of grooves and a modified Rayleigh number equal to $Ra_m = 10^5$. Generally, when setting the height h of the grooves the heat exchange rate decreases with the number of blocks. For a fixed number of grooves, the heat transfer rate decreases with the increase of the height h of the blocks. For the cases studied, the best geometric configuration is that corresponding to three grooves.

In Fig. 10, we represent the temperature profile along the heated portion for different modified Rayleigh number. We see that the temperature increases with the modified Rayleidh number. The temperature also increases at the passage of each protuberance and then decreases.

Fig. 11 show the variation of the mass flow rate in function of the height h of the grooves for a modified Rayleigh number equal to $Ra_m = 10^5$ and for different numbers of obstructions. The effect of the number of grooves on the mass flow is detectable only from a fixed height. In fact, beyond this value, curves separate and the flow rate increases according to the number of grooves.

Fig. 12 shows the streamlines for a modified Rayleigh number equal to $Ra_m = 10^5$ and for a height h equal to h = 0.0625 when the mass flow rate M is minimum. We note that the streamlines remain parallel. However, a small deformation of these lines is observed because of the penetration of the fluid into the cavities. We also note the formation of a penetration

ISSN 2356-5608

zone of the side of the adiabatic wall of the channel. This causes a folding of the streamlines on the side of the hot wall. Fig. 13 shows the streamlines for a modified Rayleigh number equal to $Ra_m = 10^5$ and for a height h equal to h = 0.5 when the mass flow rate M is maximum. Fluid enters the cavities; there is formation of two vortex counter rotating on the side of the wall before each block. These two vortices are of different sizes: the vortex at the inlet of the cavity is small while that at the bottom is larger. We also note that the size of the vortices increases from the second to the last hurdle. We also note a strong deformation of the penetration zone following the increase of the Rayleigh number.

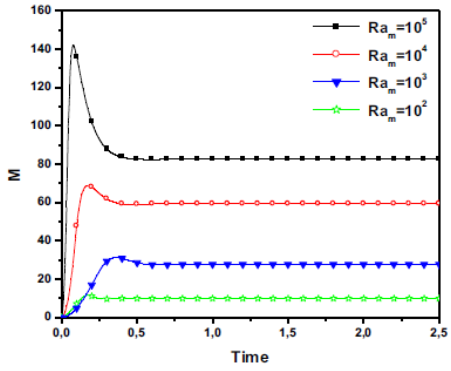

Fig. 4 Time variation of the non-dimensional mass flow rate for different modified Rayleigh numbers

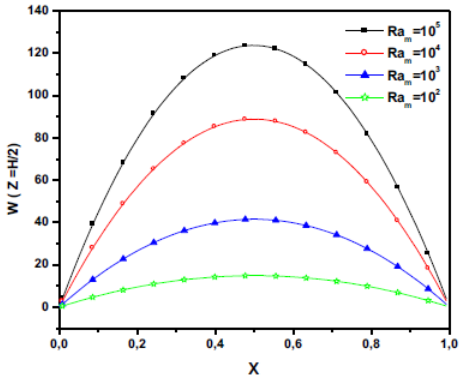

Fig. 5 Vertical velocity profiles at the entrance of the channel for various modified Rayleigh numbers

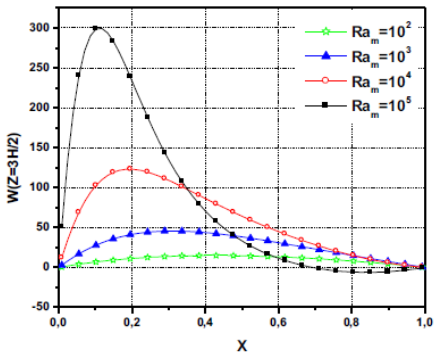

Fig. 6 Vertical velocity profiles at the exit of the channel for various modified Rayleigh numbers

Table 1: improvement of the mass flow rate in a channel $Ra_m=10^5$

$Ra_m=10^5$	3 obstructions	4 obstructions	3 obstructions	5 obstructions
h=0,125	4,35%	4,22%	4,18%	22,58%
h=0,25	8,52%	8,25%	8,16%	35,42%
h=0,375	14,06%	12,93%	10,83%	42,72%
h=0,5	19,54%	17,06%	14,34%	45,57%

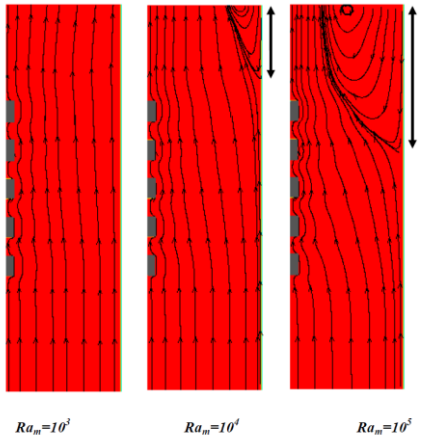

Fig. 7 Streamlines for different modified Rayleigh numbers Ra_m (h = 0.0625)

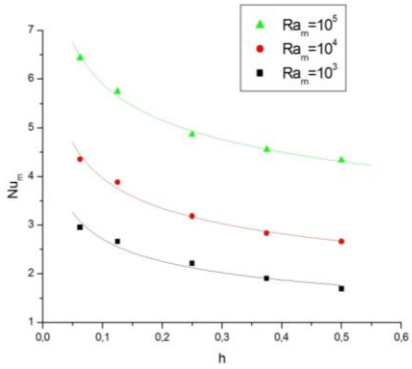

Fig. 8 Variation of the average Nusselt number as a function of the height h for different modified Rayleigh numbers

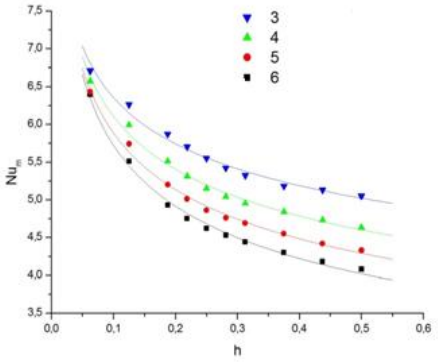

ISSN 2356-5608

Fig. 9 Variation of the average Nusselt number as a function of the numbers of obstructions

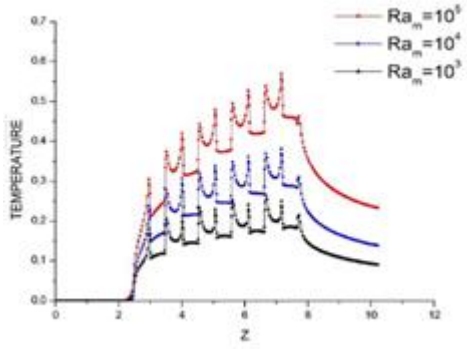

Fig. 10 Variation of the temperature for different modified Rayleigh numbers

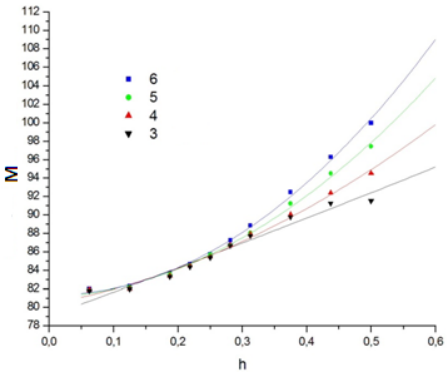

Fig. 11 mass flow rate in function of the numbers of slots for different heights ($Ra_m=10^5$)

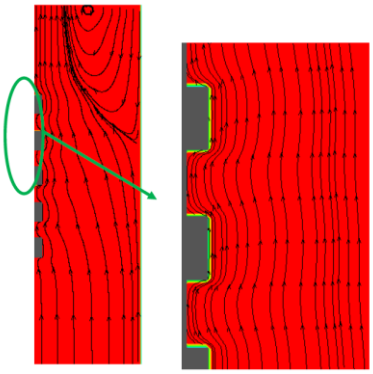

Fig. 12 Streamlines for a modified Rayleigh number equal to $Ra_m=10^5$ (h=0.0625)

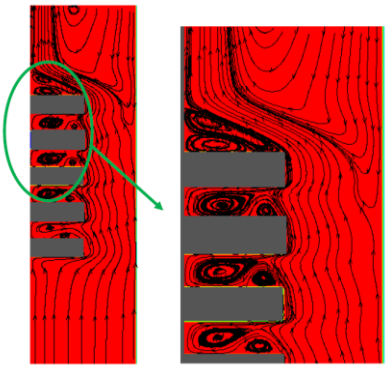

Fig. 13 Streamlines for a modified Rayleigh number equal to $Ra_m=10^5$ (h=0.5)

V. Conclusion

Study of natural convection in a corrugated vertical channel has been made for an air flow in laminar conditions.

To study the impact of the geometry of rectangular grooves on improving the heat transfer, our numerical simulations were performed for a wide range of geometric and physical parameters such as the number, the size of grooves and Rayleigh number.

The results obtained show that the increase of Rayleigh number generally results in an improved heat transfer rate, but at different degrees depending the geometry.

Finally, we can conclude that the geometric parameters have a significant influence on the heat transfer rate.

Thanks

This work was performed in the laboratory of Mathematical and Physical LAMPS in collaboration with the Laboratory of Energy and Thermal Transfer and Mass flow LEETM, within the team Bizerte in the Faculty of Sciences in the framework of thesis under joint supervision of the University of Perpignan Via Domitia in France and the University of Carthage in Tunisia.

Nomenclature

H	height of the heated wall (m)
d	channel width (m)
g	gravity acceleration (m s^{-2})
h	obstruction width (m)
M	mass flow rate
Nu	Nusselt number
Nu_m	average Nusselt number
P	pressure (Pa)
Pr	Prandtl number
Ra	Rayleigh number
Ra_m	modified Rayleigh number
Q	heat flux (W m^{-2})
*	adimensional variables

References

[1] W. Elenbaas, Heat dissipation of parallel plates by free convection. Physica 9 (1942) 1-28. Holland.

[2] J.R. Bodia, J.F. Osterle, The development of free convection between heated vertical plates, Journal of Heat Transfer 84 (1962) 40-44.

ISSN 2356-5608

[3] W. Aung, Development of laminar free convection between vertical flat plates with asymmetric heating, International Journal of Heat and Mass Transfer 15 (1972) 2293-2308.

[4] Vajravelu, Sastri, Correction to "Free convection effect on the oscillatory flow past an infinite, vertical, porous plate with constant suction. I", Proceedings of the Royal Society of London. Series A, Mathematical and Physical Sciences 353 (1673) (Mar. 25, 1977) 221-223.

[5] Sparrow, Natural convection in vertical channel: I. Interacting convection and radiation, II. The vertical plate with and without shrouding, Numerical Heat Transfer 3 (1980) 297-314.

[6] Webb, Hill, High Rayleigh number laminar natural convection in an asymmetrically heated vertical channel, Journal of Heat Transfer 111 (1989) 649-656.

[7] D. Naylor, J.M. Floryan, J.D. Tarasuk, A numerical study of developing free convection between isothermal vertical plates, Transactions of the ASME Journal of Heat Transfer 113 (1991) 620-626.

[8] K.T. Lee, Natural convection in vertical parallel plates with an unheated entry or unheated exit, Numerical Heat Transfer A 25 (1994) 477-493.

[9] A. Campo, O. Manca, B. Morrone, Numerical analysis of partially heated vertical parallel plates in natural convective cooling, Numerical Heat Transfer A 36 (1999) 129-151.

[10] Haaland, Sparrow, Mixed convection plume above a horizontal line approach flow, International Journal of Heat and Mass Transfer 26 (3) (1983) 433-444.

[11] P.H. Oosthuizen, A numerical study of laminar free convective flow through a vertical open partially heated plane duct, ASME HTD 32 (1984) 41-48.

[12] B. Morrone, O. Manca, Numerical analysis of natural convection in symmetrically heated vertical channels with an auxiliary parallel plate, in: Int: NHTC-HTD/117, Albuquerque, NM, USA, ASME, 1999

[13] A. Auletta, O. Manca, B. Morrone, V. Naso, Heat transfer enhancement by the chimney effect in a vertical isoflux channel, International Journal of Heat and Mass Transfer 44 (2001) 4345-4357.

[14] Auletta, Thermal design of symmetrically and asymmetrically heated channelchimney systems in natural convection, Applied Thermal Energy 23 (2003) 605-621.

[15] A. Andreozzi, Numerical study of natural convection in vertical channels with adiabatic extensions downstream, Numerical Heat Transfer A 47 (2005) 1-22.

[16] A. Andreozzi, O. Manca, Thermal and fluid dynamic behavior of symmetrically heated vertical channels with auxiliary plate, Int. J. Heat Fluid Flow 22 (2001) 424-432.

[17] S. Taieb, A.H. Laatar, J. Balti, Natural convection in an asymmetrically heated vertical channel with an adiabatic auxiliary plate, Int. J. Therm. Sci. 74 (2013) 24-36.

[18] G. Tanda, Natural convection heat transfer in vertical channels with and without transverse square ribs, Int. J. Heat Mass Transfer 40 (1997) 2173-2185.

[19] G. Desrayaud, A. Fichera, Laminar natural convection in a vertical isothermal channel with symmetric surface-mounted rectangular ribs, Int. J. Heat Fluid Flow 23 (2002) 519-529.

[20] W. Kim, and R. F. Boehm, Combined free and forced convective heat transfer from multiple rectangular wall blocks in vertical channels. In Mixed Convection And Environmental Flows**,** ASME HTD-Vol. 152, pp. l-8 (1990).

[21] S. Habchi, and S. Acharya, Laminar mixed convection in a partially blocked, vertical channel, Int. J. Heat Mass Transfer 29, 1711-1722 (1986).

[22] ***S.*** A. M. Said, and R. J. Krane, An analytical and experimental investigation of natural convection heat transfer in vertical channels with a single obstruction, Inl. J. Heat Mass Transfer 33, 1121-I 134 (1990).

[23] S. A. M. Said, and A. Muhanna, Investigation of natural convection in a vertical parallel-walled channel with a single square obstruction. In Simulation And Numerical Methods in Heat Transfer, ASME HTD-Vol. 153, pp. 73-80 (1990).

[24] A. Mehrotra and S. Acharya, Natural convection heat transfer in smooth and ribbed vertical channels, Znt. J. Heat Mass Transfer 36,236-241 (1993).

[25] A.H. Laatar, M. Benahmed, A. Belghith, P. Le Quéré, 2D large eddy simulation of pollutant dispersion around a covered roadway, Journal of Wind Engineering and Industrial Aerodynamics 90 (2002) 617-637.

[26] M. Bouterra, A. El Cafsi, A.H. Laatar, A. Belghith, P. Le Quéré, Simulation numérique bidimensionnelle d'un écoulement turbulent stratifié autour d'un obstacle, International Journal of Thermal Sciences 41 (3) (2002) 281-293.

[27] Z. Mahrez, M. Bouterra, A. El Cafsi, A. Belghith, P. LE Quéré, Mass transfer control of a backward-facing step flow by local forcing e effect of Reynolds number, Thermal Science 15 (2) (2011) 367-378.

[28] A. Sergent, P. Joubert, S. Xin, P. Le Quéré, Resolving the stratification discrepancy of turbulent natural convection in differentially heated air-filled cavities Part II: End walls effects using large eddy simulation, International Journal of Heat and Fluid Flow 39 (February 2013) 15-27.

[29] P. Le Quéré, On the computation of some external or partially enclosed natural convection flows, in: Proceedings of ICCHMT 2011 – 7th International Conference on Computational Heat and Mass Transfer, Istanbul, Turkey, 2011.

ISSN 2356-5608